ESTEEM Academic Journal
Vol. 13, June 2017, 39-54

EXPERIMENTAL STUDY OF DUCTILITY ADEQUACY ON INTERIOR WALL-SLAB JOINT SUBJECTED TO LATERAL CYCLIC LOADING

Mohd Ashaari bin Masrom[1*], Nor Hayati binti Abdul Hamid[2] and Mohd Elfie bin Mohamad[2]

[1]*Faculty of Civil Engineering, Universiti Teknologi MARA (UiTM) MALAYSIA, 13500 Permatang Pauh, Penang, Malaysia*
[2]*Faculty of Civil Engineering, Universiti Teknologi MARA (UiTM) MALAYSIA, 40450 Shah Alam,Selangor , Malaysia*

**Corresponding author: ashaarimasrom@ppinang.uitm.edu.my*

ARTICLE HISTORY

Received
5 January 2017

Received in revised form
6 June 2017

Accepted
20 June 2017

ABSTRACT

In Malaysia, the tunnel-form building has been utilised in building construction since 1980 in the construction of high-rise residential house such as condominium and apartment. Most of the tunnel-form buildings have been designed according to British Standard (BS) whereby there is no provision for seismic loading. The high-rise tunnel-form building is vulnerable to seismic loading and the joint between slab and shear walls in tunnel-form building constitute an essential link in the out-of-plane lateral load-resisting mechanism. It is a known fact that Malaysia is no longer safe from earthquake disaster consequent to the damage of building. The ductility performance of interior wall-slab joint influences the pattern and distribution of lateral forces among the vertical elements of a structure. In line with that, this study presents the results of an experimental investigation on the ductility performance of interior wall-slab joint which is designed in accordance to BS 8110.The experiment work includes a full-scale test of wall-slab joint sub-assemblages under out-of-plane lateral cyclic loading. One sub-assemblage specimen of the interior wall-slab joint was designed and constructed according to the code. The specimen was tested based on lateral displacement control (drift control). It was found that the specimen is able to survive up to 1.5% drift. The analysis results indicate that the specimen was governed by brittle failure modes with ductility class low (DCL) as stated in Eurocode 8 (EC8). This resulted from insufficient reinforcement provided. Consequently, the specimen was unable to dissipate sufficient energy to sustain longer in the inelastic zone.

Keywords: hysteresis loops; wall–slab joint; equivalent viscous damping; lateral cyclic loading;

p-ISSN 1675-7939; e-ISSN 2289-4934

1. INTRODUCTION

One of the major issues that arises in the designing of high-rise reinforced concrete (RC) building is concerned with the lateral resistance of building to resist the lateral force which commonly comes from wind and earthquake loading. However, nowadays wind loading is not the major problem which caused the collapse of the building. Many codes of practice were developed to accommodate wind load factor to determine structural integrity and stability of RC buildings. Meanwhile, the seismic load is the loading that always impairs the building structure and causes the holocaust such as the collapse of the building. There are many earthquake events in Indonesia which caused tremors to the people who live in high-rise buildings in Malaysia. For instance, the earthquake with a magnitude of 7.9 scales Richter recorded in September 2009 in South Sumatera, Indonesia in which had resulted tremors in the few areas in the west coast of Peninsular Malaysia. It was reported that many Malaysians especially those who stay in high-rise building felt the swaying of the building after the earthquakes struck in Indonesia. Recently, the earthquake struck in Ranau, Sabah in 2015. It was reported some infrastructure damages which included around 25 schools in six different districts affected and Ranau Mosque damaged due to the tremor. Serious damages occurred to the hostels and rest house near the summit of the Mount Kinabalu. It was discovered through an inspection that 30 percent out of 65 buildings in the entire country inclusion of Kuala Lumpur, Putrajaya, and Klang are vulnerable to earthquake risk. In fact, less than one percent of the buildings in Malaysia comply with the specification of seismic resistance. Due to a rapid demand on the residential apartment in Malaysia, most of the high-rise buildings in Malaysia are constructed using tunnel-form buildings. Most of the buildings in Malaysia were designed according to BS8110 where there are no provisions for earthquake loading at all. Therefore, it is expected that most of these buildings will suffer moderate or severe damages if the magnitude of an earthquake more than 6.5 scales Richter strike Malaysia. In relation to that, the numbers of researchers in Malaysia that have undertaken an investigation on the seismic performance of structures using existing designed code is on the rise. For instance, Yee et. al (2011) reviewed on the performance of IBS precast concrete beam-column connections under earthquake effects in Malaysia. This was followed by Masrom et. al (2012) who studied on the seismic performance of exterior wall-slab joint. He found that the joint was governed by brittles modes. Further, Ghani et. al (2013) have undertaken an investigation of non-seismic precast RC beam-column exterior joint under lateral cyclic loading. Anuar et. al (2015) have carried out a laboratory works on the tunnel-form building subjected to lateral cyclic loading. In addition to that, Masrom et.al (2016) undertook a seismic behaviour of unrepaired and repaired tunnel-form-building under in-plane lateral cyclic loading. It was discovered that a very limited research study has been carried out about the interior wall-slab joint. It has been started by Pantazoupouloul et. al (1992). They have carried out the laboratory works on the wall-slab connection subjected to in-plane lateral cyclic loading. Kudzys (1996) carried out a finite element study to evaluate the wall-slab connection behaviour under extreme lateral actions. Further, Kaushik et. al (2016) carried out a nonlinear time history analyses, under different levels of recorded earthquake ground motion using the

p-ISSN 1675-7939; e-ISSN 2289-4934

computer program ABAQUS to study the seismic damage in shear wall – slab junction of an RC wall-frame building. To date, it was found that no specified study has ever undertaken to investigate the seismic performance of physical interior wall-slab joint subjected to out-of-plane cyclic loading. The joint between slab and shear walls in tunnel-form building constitute an essential link in the out-of-plane lateral load-resisting mechanism. Therefore, this study intended to investigate the survivability of the interior wall-slab joint designed to British Standard under seismic loading.

2. THEORETICAL BACKGROUND

2.1 Quantifying ductility from the experiment

Ductility can be defined as the ability of a material to deform subjected to an inelastic region within acceptable stiffness and strength reduction (Park & Paulay, 1975). Ductility is a significant consideration that may add to the strength and serviceability of a structure under continuous loading. A ductile structure must be able to dissipate energy during cyclic deformations. According to Park and Paulay (1975), ductility estimation is an important parameter to ensure that the structure cannot fail in brittle fashion without warning during extreme events such as earthquakes. The structure must also be able to cater for larger deformations at near maximum load carrying capacity. It is meaningful to say that the ductility factor is defined as the ultimate deformation divided by the corresponding deformation present at the yield point (Park, 1988). Figure 1 shows the idealised elastoplastic behaviour of the displacement ductility factor (μ_Δ) . The displacement ductility factor can be derived as equation 1.

$$\mu_\Delta = \frac{\Delta_u}{\Delta_y} \tag{1}$$

where Δ_u is the ultimate displacement and Δ_y is the displacement at yield.

p-ISSN 1675-7939; e-ISSN 2289-4934

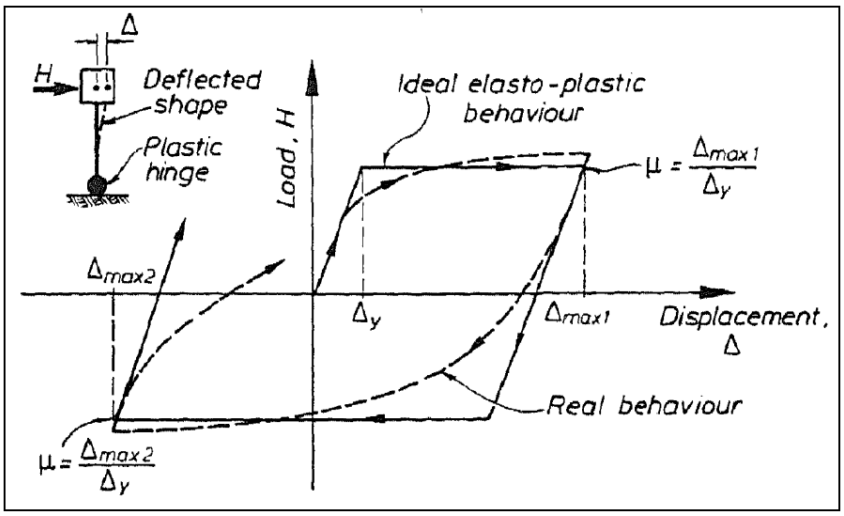

Figure 1: Displacement Ductility Factor (Park, 1988)

In this study, the definition of displacement of yield is adopted from Park (1988) as shown in Figure 2. It is the most realistic definition for the yield displacement for reinforced concrete structures. Based on reduced stiffness equivalent elastoplastic yield, the yield displacement was found to be 75% of the ultimate lateral load, H_u. This definition includes the reduction of stiffness due to the cracking near the end of the elastic range.

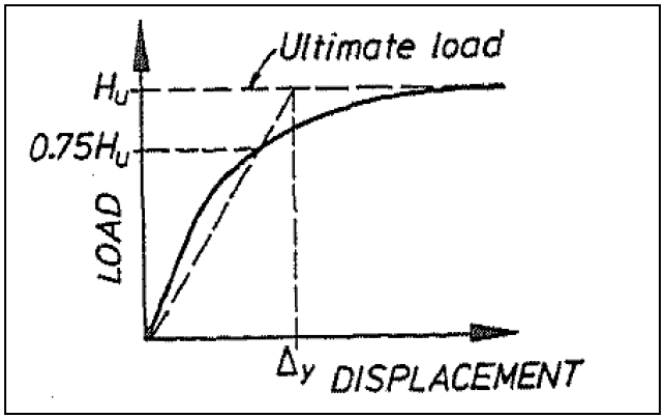

Figure 2: The Realistic Definition of Yield Displacement (Park, 1988)

There are several alternative definitions of ultimate displacement (Δ_u); the most realistic ones are given by the criteria shown in Figure 3. The ultimate displacement can be estimated as that post-peak deformation when the load has been reduced by a small specified amount as shown in Figure 3 (a). The drop-in strength is commonly taken as 20% (Priestley et al., 2007) from the peak load or maximum attained strength. The maximum ultimate displacement can also be obtained when the reinforcement fractures or buckles as shown in Figure 3(b). These two definitions are used to estimate the maximum ultimate displacement, whichever occurred first.

p-ISSN 1675-7939; e-ISSN 2289-4934

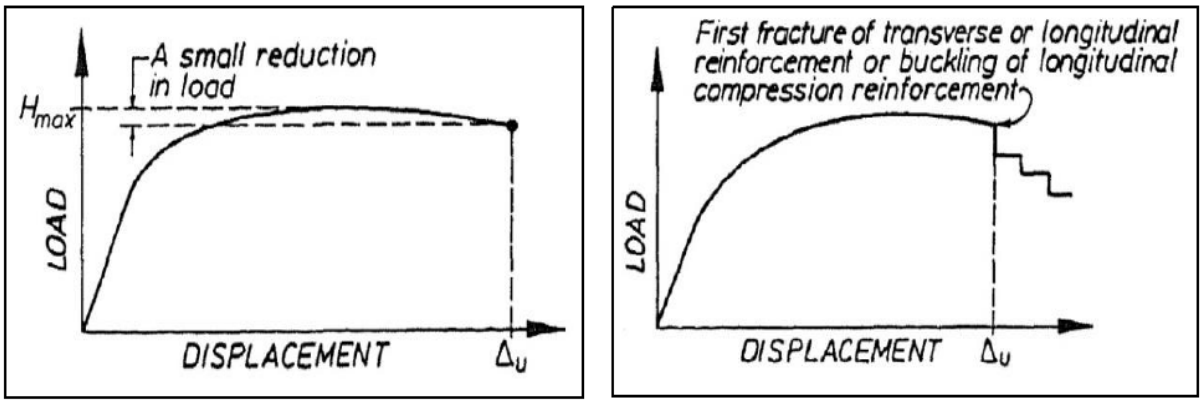

(a) Based on significant load capacity after peak load (b) Based on fracture or buckling of reinforcement

Figure 3: Definitions for Maximum Ultimate Displacement (Park, 1988)

2.2 Quantifying ductility from the analytical equation

The curvature ductility of reinforced concrete can be quantified by using equation 2. This equation was derived by considering the strain diagram of reinforced concrete under yield and ultimate state as depicted in figure 4. The derivation works of this equation can be obtained from Indian Standard (IS 456, 2000).

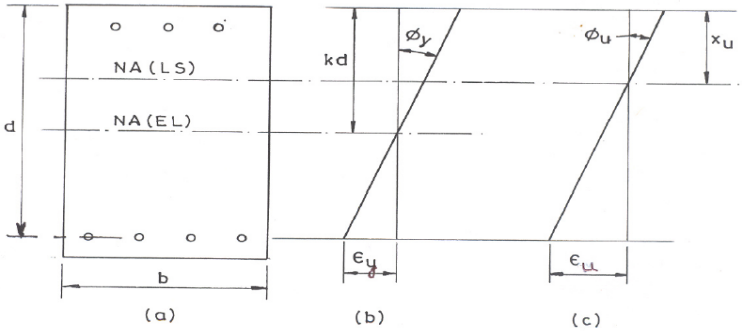

Figure 4: (a) Cross section, (b) During yield, (c) At ultimate state

$$\mu_{\emptyset} = \frac{\varepsilon_u}{f_y/E_s}\left(\frac{1+mp-\sqrt{m^2p^2+2mp}}{x_u/d}\right) \tag{2}$$

The equivalent displacement ductility, μ_{Δ} can be determined based on the analytical formula derived by Park and Paulay (1975) as shown in equation 3.

$$\mu_{\Delta} = 1 + \left(\frac{\emptyset_u - \emptyset_y}{\emptyset_y}\right) 3l_p \left(\frac{l-0.5l_p}{l^2}\right) \tag{3}$$

where $$\emptyset_y = \frac{\varepsilon_y}{d-kd} \quad \text{and} \quad \emptyset_y = \frac{\varepsilon_u}{x_u}$$

The plastic hinge length, l_p can be determined based on Baker, (1956).

p-ISSN 1675-7939; e-ISSN 2289-4934

3. METHODOLOGY

3.1 Construction of Interior Wall-slab Sub-assemblage

The simulation work was conducted prior the laboratory testing. This was done to ensure the behaviour of the sub-assemblage specimen that was going to be constructed in the laboratory would reflecting the actual condition of the interior wall-slab joint in the tunnel-form structure under lateral cyclic load.

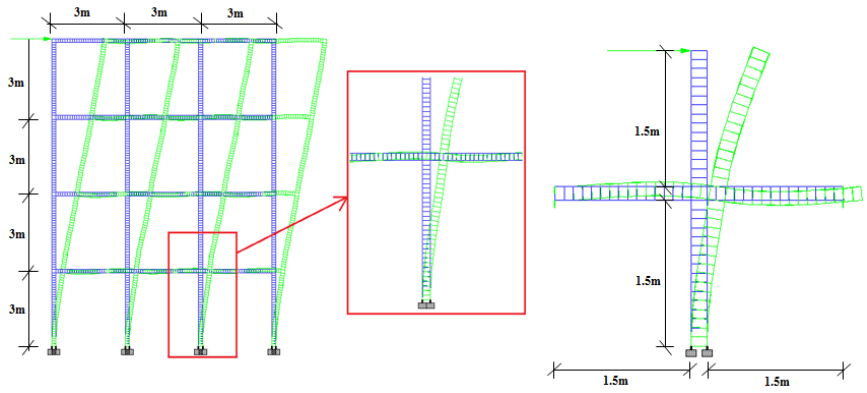

(a) prototype model (tunnel-form structure) (b) sub-assemblage model

Figure 5: Simulation of the sub-assemblage joint against the prototype model (tunnel-form structure)

The inter-storey height of the wall and the floor span to form a tunnel-box was 3m by 3m size. Meanwhile, the shear wall height and floor span for the sub-assemblage model have been adopted based on the half length of the prototype model. It was found that the deformation shape of the sub-assemblage model towards the five-storey prototype model at the interior joint of wall-slab was identical by comparing Figure 5(a) and (b).

The sub-assemblage specimen of interior wall-slab joint comprised the foundation, shear wall and slab panels as shown in Figure 6.0. Based on the laboratory constraint, the height of the wall panel was limited to 1800mm while the length of slab panel was 1500 mm measured from the wall surface. The thickness of all panels was 150mm. The length, width and thickness of foundation beam are 1800mm, 965mm, 325mm respectively. This specimen has been designed according to British Standard (BS8110, 1997) with grade 30 concrete.

p-ISSN 1675-7939; e-ISSN 2289-4934

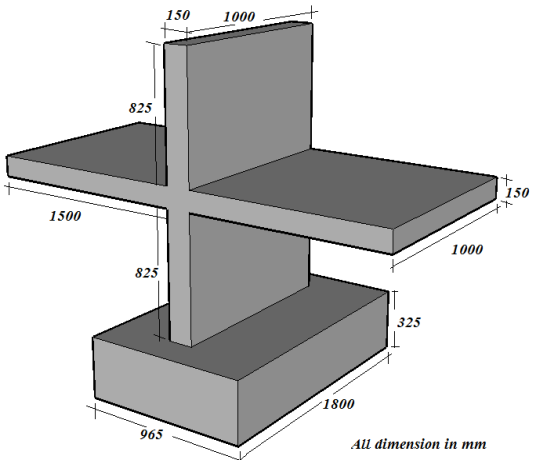

Figure 6: Schematic diagram of Interior Wall-slab joint design to British Standard

The reinforcements comprised fabric wire mesh (BRC-7) and high yield reinforcement bars of 16 mm diameter with yield strength, f_y of 460N/mm^2. Figure 7 shows the reinforcement detail at the interior wall-slab joint. Fabric wire mesh (BRC-7) with 200mm by 100mm grid has been utilised. The arrangement of the wire mesh in the specimen can be seen in this figure. Hogging bars of 12mm diameter have placed 100mm apart in the transverse direction to cater negative moment in the slab panels.

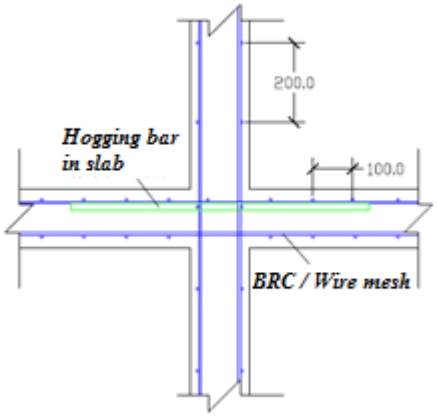

Figure 7: Reinforcement detail of Interior Wall-slab joint (dimension in mm).

Figure 8 and 9 show the photo of joint reinforcement and the completed specimen respectively.

p-ISSN 1675-7939; e-ISSN 2289-4934

Figure 8: Reinforcement detail of Interior Wall-slab joint

Figure 9: Configuration of the specimen under testing

3.2 Instrumentation and Experimental Set-up

Figure 10 shows the systematic arrangement of linear potentiometers and double actuator. The load cell with a capacity of 250kN was connected to double actuator and supported by the reaction frame. The double actuator has imposed the lateral cyclic loading on the wall with control displacement. While the head of the load cell was connected to a steel plate and clamped to the wall by having the treaded bars screwed up and snugly tight.

p-ISSN 1675-7939; e-ISSN 2289-4934

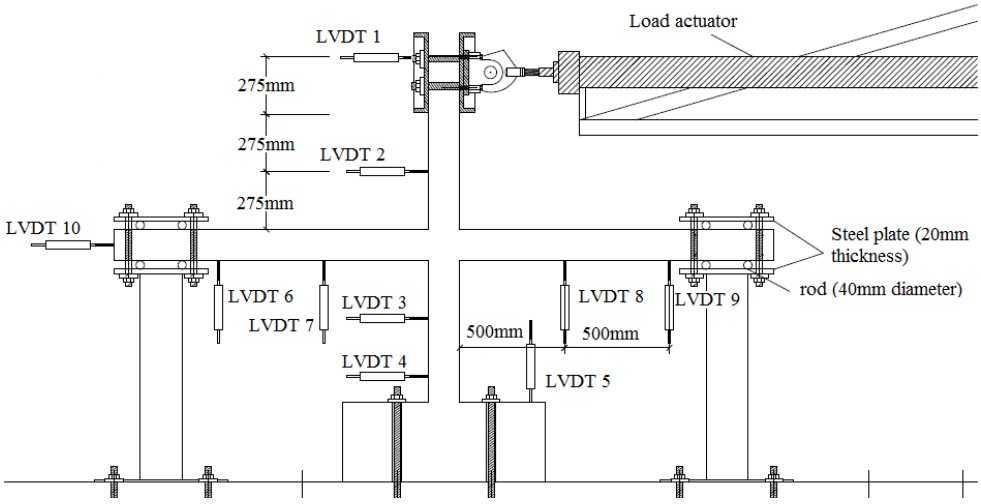

Figure 10: Schematic diagram of Experimental set-up of specimen

The RC wall became sandwiched by steel plate clamping to the double actuator head so that the wall can be pushed and pulled laterally during the experiment. The end slab panels of the specimen were supported by the roller. This roller support was demonstrated by putting a rod at above and bottom of end slab panels. These rods were allowed to roll over horizontally in between the slab panels and fabricated sandwiched plate as depicted in figure 10. The foundation beam was clamped to the strong floor by penetrating the high yield threaded bar through the holes located in foundation beam. A total number of 10 LVDT have been installed on the specimen in order to record the deflection consequential from the lateral cyclic load applied on the sample. Five units of LVDT have been installed horizontally along the height of wall while another five units along the slab span and foundation as depicted in Figure 10. Strain gauges have been installed to monitor and capture the change in strain of reinforcement due to alternate tension and compression strain during the experiment work. The strain gauges at reinforcement bar had been installed prior to the cast of the sample. The detail arrangement of strain gauges on the reinforcement joint can be seen in Figure 11.

p-ISSN 1675-7939; e-ISSN 2289-4934

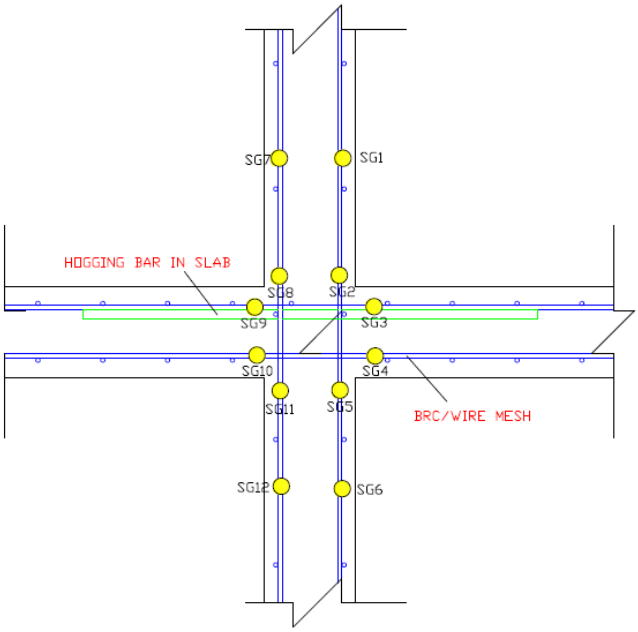

Figure 11: Location of strain gauges at the wall-slab joint

3.3 Testing Procedure and Loading Regime

Figure 12 shows the loading regime procedure adopted from ACI ITG-5.1-07 (2007). The specimen was loaded with a hydraulic actuator having 250 KN capacities through a load cell with lateral displacements control. The push and pull load has been applied in full two cycles at each drift level. At each incremental of displacement, the maximum load was maintained constant for a few seconds in order to measure and record the load, displacement response of the walls and the steel strain via electronic data logger. The loading applied on top of wall specimen comprised quasi-static lateral displacement control based cycles. Initial cycles starting with ± 0.1% and ±0.25% lateral drift were completed for two cycles for each drift. These cycles were within the elastic range which allowed the stiffness and yield displacement of the joint to be established. Subsequent cycles were composed of large increment amplitudes. Lateral displacement applied should be slowly and steady so that the pattern of hysteresis loops can be obtained. The application of the lateral displacement and loading were at a height of 1800 mm above the strong floor. This schedule was completed up to 1.5% lateral drift.

p-ISSN 1675-7939; e-ISSN 2289-4934

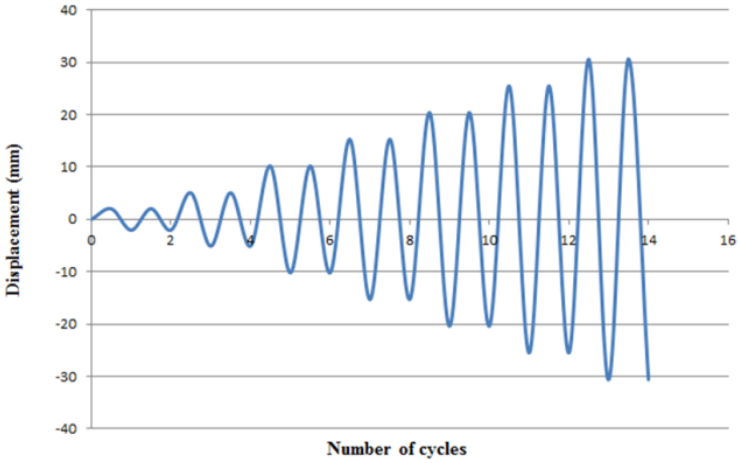

Figure 12: Testing schedule for BS wall-slab joint

The damage was identified based on a number of cracks, spalling of concrete, buckling of reinforcement bars and fracture of bars. It is crucial to monitor the behaviour of steel during elastic, yield plateau, elastoplastic and ultimate or failure load.

4. EXPERIMENTAL RESULTS AND VISUAL OBSERVATIONS

4.1 Cracks Propagation on Specimen

All the cracks have undergone opening and closing during the experiment due to alternate compression and tension stress generated by the lateral cyclic loading. These cracks were opened by tension stress while closed by compression stress. The cracks were visible in the early of 0.1% drift level at wall-slab joint, upper wall and slab panel. These cracks have continued propagated up to 0.5% in those regions. It was found that the wall-slab joint has started to lose its fitting against the upper wall panel within 0.75% to 1.0%. This behaviour can be observed graphically in Figure 13.

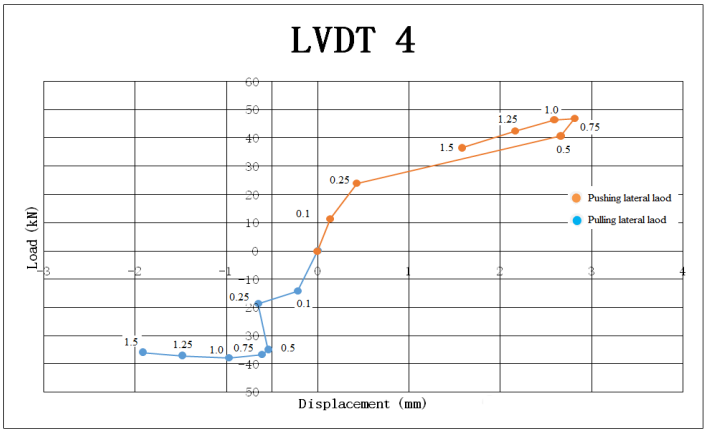

Figure 13: Lower wall load-displacement response of specimen at LVDT 4

p-ISSN 1675-7939; e-ISSN 2289-4934

According to Figure 13, the displacement of the lower wall has begun to drop at 1.0% drift. This indicates that the joint between upper walls against specimen has started to break. Approximately, at 0.75% drift, the concrete wall was broken and the enlargement of cracks has continued to penetrate towards wall reinforcement.

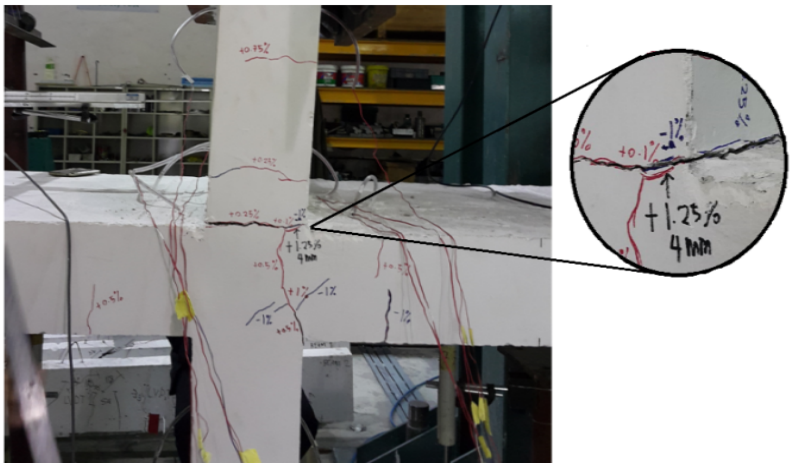

Figure 14: Visual observation of cracks propagated on interior wall-slab joint within 1.25% to 1.5% drift level

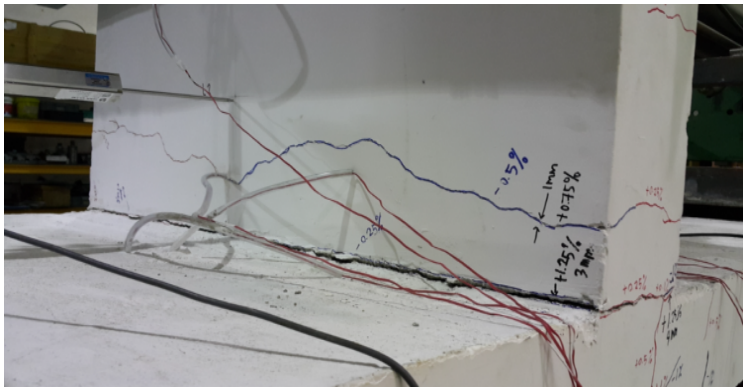

Figure 15: Wall-slab joint view from side

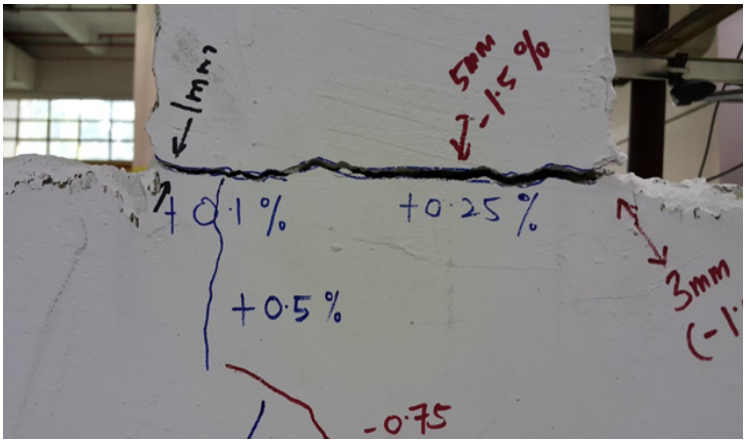

Figure 16: Fracturing of upper wall panel

p-ISSN 1675-7939; e-ISSN 2289-4934

The slab panels to the upper wall panel were connected effectively up to 0.75% drift and lost their connection when reaching 1.0% drift. No more new cracks have been propagated on wall and slab panels beyond 1.0% indicating that the surface stresses have reduced in the entire specimen. The significant enlargement of cracks has observed in between upper wall to the wall-slab joint at 1.25% drift as depicted in Figure 14, 15 and 16.

4.2 Hysteresis Loop and Ductility Capacity

Figure 17 illustrates the hysteresis loop of the specimen at LVDT 1 that was superimposed by the equivalent monotonic pushing/pulling load-displacement response. This has signified that the dynamic response of wall-slab joint resembles the static behaviour that is commonly encountered in the reinforced concrete structures. The strength degradation of the joint can be observed clearly in this figure. The ultimate capacity of lateral resistance of the specimen was 46.9 kN at 0.75% drift. The joint behaved elastically up to 0.25% drift. Yielding has been found to take place on the first cycle to ± 0.25% drift at about 24kN lateral force. In this study, the definition of displacement of yield and the ultimate displacement were determined based on theoretical background.

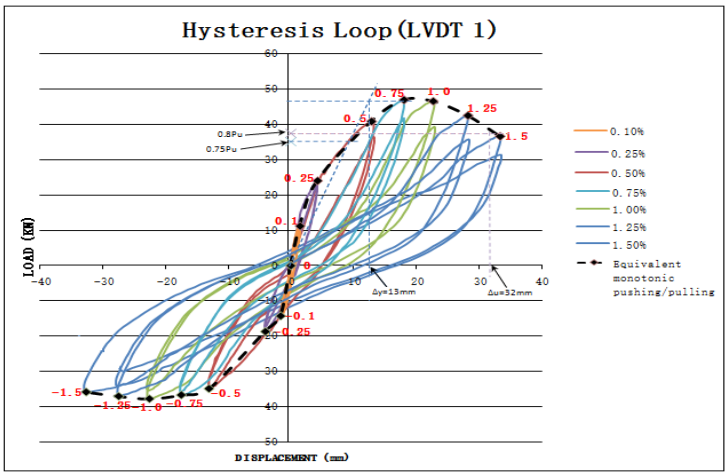

Figure 17: Upper wall peak load-displacement response of specimen at LVDT 1.

The experimental ductility was calculated according to equation 1. Consequently, the ductility, μ capacity of this unit was 32/13=2.5. It was found that the displacement ductility calculated from the analytical formula from equation 3 was equal to 2.34 which showed acceptable agreement with respect to experimental value. The accepted range of ductility which was specified in Eurocode 8 is 3 to 6 for Ductility Class Medium (DCM). The calculated displacement ductility for specimen was less than 3 and it was classified as Ductility Class Low (DCL) as stated in Eurocode 8 (EN1998). Consequently, the interior wall-slab joint designed according to BS 8110 will not survive under moderate to strong earthquake events.

p-ISSN 1675-7939; e-ISSN 2289-4934

5. CONCLUSION

Based on the analysis of results, discussion, and visual observation during the experiment, the following conclusions can be drawn as follows:

1) The interior wall-slab joint has undergone four major states during the experiment, which are cracking, yielding, ultimate and fracturing state.
2) Approximately, the joint has yielded at 0.25% drift and reached the ultimate state at 0.75% drift. Beyond 0.75% drift, the joint has failed and ultimately fractured at 1.5%.
3) The calculated displacement ductility for specimen was less than 3 and it is classified as Ductility Class Low (DCL) as stated in Eurocode 8.
4) Insufficient reinforcement provided in the interior wall-slab joint consequent low ductility that leads to brittle failure modes of the joint as depicted in Figure 16. The joint could not sustain longer in the plastic zone after it yielded.
5) The specimen was unable to dissipate sufficient energy to sustain longer under inelastic deformation.
6) The BS8110 code is no longer realistic to be adopted in designing the tunnel form-building based on the current seismic demand in Malaysia.

ACKNOWLEDGEMENT

The authors would like to thank the Research Management Institute, University Teknologi MARA Pulau Pinang, Malaysia and the Ministry of Higher Education, Malaysia for the funding [Ref. No Ref. No 600-RMI/RAGS 5/3 (179/2014)] this research works under Research Acculturation Grant Scheme (RAGS). Nevertheless, the authors also want to express their gratitude to the technicians of Heavy Structures Laboratory, Faculty of Civil Engineering, UiTM for conducting this research work successfully.

REFERENCES

Anuar, S.A., Hamid,N.H., & Hashim, M.H. (2015). Strengthening of single bay tunnel-form building using steel angle, steel plate and CFRP under out-of-plane cyclic loading. Proceedings of 2015 *International Conference on Disaster Management in Civil Engineering*, Universal Researchers, 21-26.

ACI Innovation Task Group 5 (2007). *Acceptance Criteria for Special Unbonded Post-Tensioned Precast Structural Walls Based on Validation Testing (ACI ITG 5.1-07) and Commentary*. American concrete Institute, Farmington Hills, MI.

Baker, A.L.L. (1956). 'Ultimate Load Theory Applied to the Design of Reinforced and Prestressed Concrete Frames'. Concrete Publications Ltd, London.

BS8110: Part 1 (1997). *Structural Use of Concrete. Part I: Code of Practice for Design and Construction.* British Standards Institution, UK.

p-ISSN 1675-7939; e-ISSN 2289-4934

EN1998: Part 1 (1998). *General rules, seismic actions and rules for buildings*. European Standard Institution, UK.

Ghani, K.D., & Hamid, N.H. (2013). Experimental Investigation on a non-seismic precast RC beam-column exterior joint under quasi-static lateral cyclic loading. *Safety and Seismic Engineering V*, Vol. 134, WIT Press, 827-837.

IS 456: (2000). *Indian Standard Plain and Reinforced Concrete – Code of Practice (4th Revision)*. Indian Standard, BIS, New Delhi.

Kaushik, S. and Dasgupta, K. (2016). Seismic damage in shear wall-slab junction in RC buildings. *Procedia Engineering*, Vol.144, pp. 1332–1339.

Kudzys, A. (1996). Evaluation of wall-slab connection behaviour under extreme lateral actions. Statyba, 2(8), 35-44.

Masrom, M.A., & Hamid, N.H. (2012). Ductility performance of wall-slab joint in industrialized building system (IBS) subjected to lateral reversible cyclic loading. *ESTEEM Academic Journal*, 8(1), 26-33.

Masrom, M.A., Hamid, N.H., & Anuar S.A (2016). Seismic Behaviour of Unrepaired and Repaired Tunnel Form Building Under In-Plane Lateral Cyclic Loading. *Jurnal Teknologi*, 72(1),1- 6.

Pantazoupouloul, S., & Imran, I. (1992). Slab-wall connections under lateral forces. *ACI Structural Journal*, 89(5), 515-527.

Park, R. (1988). State-of-the Art Report: Ductility Evaluation from Laboratory and Analytical Testing. Paper presented at the Ninth World Conference on Earthquake Engineering, August 2-9, Tokyo-Kyoto, Japan.

Priestley, M.J.N., Calvi, G.M., & Kowalsky, M.J. (2007). 'Displacement-Based Seismic Design of Structures'. *IIUS Press*, Pavia, Italy.

Yee, P.T.L., & Adnan, A. (2011). Performance of IBS Precast Concrete Beam-Column Connections Under Earthquake Effects: A Literature Review. *American Journal of Engineering and Applied Sciences*, 4(1), 93-101.

p-ISSN 1675-7939; e-ISSN 2289-4934

NOMENCLATURE

ε_u ultimate strain of concrete

ε_y yield strain of tensile steel

ε_{ym} maximum strain in tensile steel

μ_s strain ductility in steel

m modular ratio = $\frac{280}{\sigma_{cbc}}$

σ_{cbc} permissible stress of concrete in bending compression

l_p plastic hinge length

l length of wall

$\emptyset_y$ yield curvature

$\emptyset_u$ ultimate curvature

x_u depth of neutral axis at collapse

b width of wall

d effective depth of wall

p-ISSN 1675-7939; e-ISSN 2289-4934